Morphologic Study of Steady State Electrospun Polyamide 6 Nanofibres

Sander De Vrieze,[1] Bert De Schoenmaker,[1] Özgür Ceylan,[1] Jara Depuydt,[1] Lieve Van Landuyt,[1] Hubert Rahier,[2] Guy Van Assche,[2] Karen De Clerck[1]

[1]*Department of Textiles, Ghent University, Technologiepark 907, 9052 Gent, Belgium*
[2]*Department Physical Chemistry and Polymer Science, Vrije Univ Brussels, 1050 Brussels, Belgium*

Received 8 February 2010; accepted 27 June 2010
DOI 10.1002/app.33036
Published online 22 September 2010 in Wiley Online Library (wileyonlinelibrary.com).

ABSTRACT: Electrospinning is a process to generate a nanofibrous material. Although the working principle of electrospinning is rather straight forward, it is influenced by many parameters. There is still a serious lack of knowledge concerning the influence of the ambient parameters, for which preliminary knowledge reveals that the relative humidity is of primary importance. This article reports the influence of the relative humidity on electrospun polyamide 6 nanofibres. Mixtures of formic acid and acetic acid are used for steady state electrospinning of polyamide 6 nanofibres, for which a steady state table is determined. When the relative humidity increases, the average fiber diameter decreases and the fraction of the less stable γ-phase crystals in the polyamide diminishes. This effect is explained by absorbed water acting as a plasticizer, reducing the Tg of the polyamide. This article shows the importance of working in climatized conditions during electrospinning to obtain reproducible nanofibres. © 2010 Wiley Periodicals, Inc. J Appl Polym Sci 119: 2984–2990, 2011

Key words: electrospinning; steady state; polyamide

INTRODUCTION

Electrospinning is an innovative process, capable of producing fibers with diameters typically one to two orders of magnitude lower than extrusion and conventional solution-spun fibers. A variety of polymers can be spun, each from a specific solution. In addition, the ability to produce highly porous nanofibrous membranes with structural integrity is also an attractive feature of electrospinning.[1–3]

The concept of electrospinning was invented and patented in the beginning of the 20th century.[4–6] In the past 15 years, electrospinning experienced a renewed interest, both in academic research as well as industry. Electrospun materials offer opportunities for example in medical applications (e.g., blood vessels), filtration, and protective clothing.[7–9]

The key factor for successful nozzle electrospinning is achieving steady state conditions.[10] Electrospinning is in steady state when the amount of polymer that is transported through the needle per unit of time equals the amount of polymer that is deposited as nanofibres on the collector per unit of time. This definition comprises two conditions. The first condition is that in time all the polymer that is spun from the nozzle and collected at the target is converted into nanofibres, implying the absence of beads or drops in the structure. The second condition for steady state electrospinning is a stable, time invariant, Taylor cone. Steady state electrospinning allows for the long-term stability needed for reproducibly producing samples of any desired size. As shown in previous work, attaining steady state electrospinning conditions is possible only if the right solvent mixture is used for the selected polymer.[10] This article reports on the use of formic acid and acetic acid as a solvent mixture for the electrospinning of polyamide 6 (PA 6).

PA 6 nanofibres are generally composed of different crystal phases,[11,12] from which the α- and the γ-phase are the most common ones. The α-phase has a higher stability, resulting in a higher melting point. Because the solvent evaporation rate in electrospinning is very high, resulting in a high crystallization speed, a relatively high amount of the thermodynamically less stable γ-phase is present in PA 6 nanofibres.[11] The formation of the crystal morphology and the crystal structure is of course related to the electrospinning parameters.

Three types of parameters exist in the world of electrospinning: solution, process, and ambient parameters. The most overlooked type of parameters until now is the ambient parameters. Recent work showed the importance of ambient parameters such

Correspondence to: S. De Vrieze (sander.devrieze@UGent.be).

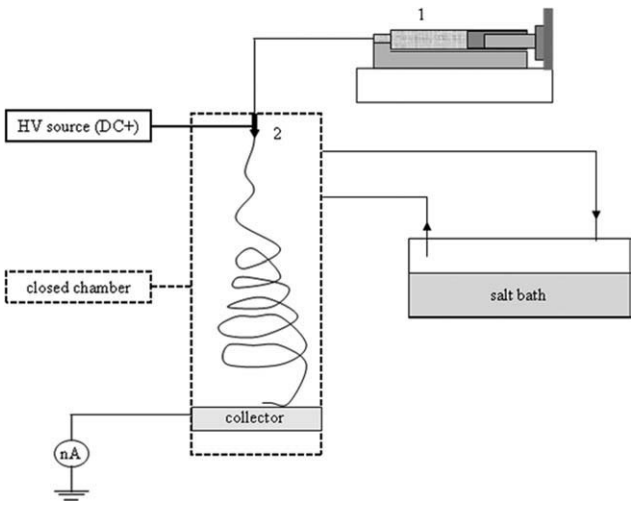

Figure 1 Scheme of the electrospinning setup, which processes a polymer solution (1) through a needle with the formation of a Taylor cone (2).

as temperature and relative humidity (RH) while electrospinning.[13] Both parameters directly influence the nanofibrous structure.

In this article, the steady state table for electrospinning PA 6 in the solvent mixture formic acid/acetic acid (FA/AA) is presented. The steady state table provides a window of solvent mixtures that allow steady state electrospinning for a defined set of process parameters. In addition, this article will focus on the effect of RH and solution composition (FA/AA ratio and polymer loading) on the crystal morphology of the nanofibrous material and the average nanofibre diameter.

EXPERIMENTAL MATERIALS

PA 6 (M_w 10000 g mol^{-1}) was supplied by Sigma Aldrich and used as received. Solvents chosen for this research were 98 wt% formic acid and 99.8 wt% acetic acid (both supplied by Sigma-Aldrich). The solutions for electrospinning were prepared by dissolving PA 6 pellets in various FA/AA solvent mixtures. The solutions were slightly stirred with a magnetic stir bar for at least 3 h at room temperature.

METHODS

Electrospinning

Figure 1 is a scheme of the electrospinning setup. The closed setup comprises an infusion pump (KD Scientific Syringe Pump Series 100) and a high-voltage source (Glassman High Voltage Series EH). A grounded aluminum foil collects the nanofibrous materials. The experiments were conducted at room temperature (20°C). A silica gel bath and a NaCl bath were used to control the RH, resulting in 15 ± 2% RH and 63 ± 2% RH, respectively. These baths were in contact with the closed electrospinning chamber through a closed system consisting of a polyvinyl chloride tube and a fan. The humidity was checked before and after an experiment and did not change significantly. A BN-1838 Terumo needle was used to perform the experiments. The high-voltage supply was capable of generating positive DC voltages directly on the needle.

Scanning electron microscope analysis

The morphology of the electrospun nanofibres was examined using a scanning electron microscope (Jeol Quanta 200 F FE-SEM) at an accelerating voltage of 20 kV. Before SEM analysis, the sample was coated with gold using a sputter coater (Balzers Union SKD 030). The diameter of a nanofibre sample was calculated by taking an average of 50 measurements.

Differential scanning calorimetry analysis

The melting of the nanofibres was studied using a Q2000 Tzero DSC from TA instruments. The instrument was calibrated using the Tzero calibration procedure, using indium, tin, and gallium for temperature and indium for heat flow calibration. Samples of ~ 3 mg placed in sealed aluminum pans were heated from 0 to 250°C at 10°C min^{-1}, under a constant nitrogen flow of 50 mL min^{-1}.

Attenuated total reflection infrared analysis

Attenuated total reflection infrared (ATR-IR) spectra were recorded with a Bruker, vertex 70 with MCT detector using a germanium ATR-crystal. For each spectrum an average of 64 scans with a resolution of 4 cm^{-1} was taken. For each sample this was done on three different locations and an average was calculated.

RESULTS AND DISCUSSION

Steady state electrospinning of PA 6

PA 6 dissolves in formic acid, but not in acetic acid. However, using pure formic acid no steady state conditions could be achieved for electrospinning PA 6. Therefore, mixtures of formic acid and acetic acid were used for electrospinning PA 6. The ratio of formic to acetic acid and polymer content (in weight percent) were varied to determine the polymer solution feeding rates resulting in a steady state electrospinning process.

The optimal steady state parameter values are summarized in Table I. This table is termed the steady state table for electrospinning of PA 6 nanofibres from

TABLE I
Steady State Table for the Electrospinning of PA 6 Nanofibres from Formic Acid and Acetic Acid Solutions: Possibility for Steady State and Corresponding Steady State Solution Flow Rates for Varying PA 6 Contents (in wt%) and Formic Acid and Acetic Acid Mixtures (v% AA) for an Applied Voltage of 30 kV and a TCD of 6 cm

	Volume fraction of acetic acid in the formic acid/acetic acid mixtures					
wt% PA 6	25 v% AA	33 v% AA	40 v% AA	45 v% AA	50 v% AA	55 v% AA
12						
13					1.5	
14			2	2.5	3	
15		2	2.5	3	4.5	
16		2.5	3	3.5	5	
17		2.5	3	3.5	5.5	
18		3	3.5	4	6.5	
19		3.5	4	4.5	7.5	
20		3.5	4	5	6.5	
21						

No steady state possible.
■ PA 6 pellets do not dissolve completely.
X Steady state flow rate for the above conditions (ml h^{-1}).

FA/AA solutions. In Table I, the applied voltage and the tip-to-collector distance (TCD) are constant at 30 kV and 6 cm respectively. These process parameters were selected, based on a first screening. For each composition for which steady state electrospinning could be reached, a single flow rate with an operating window of $\sim$ 10% results in steady state electrospinning. When the flow rate is higher than the flow rate in the table plus the operating window, drops of polyamide will be ejected out of the Taylor cone. When the flow rate is lower than the flow rate in the table minus the operating window, no Taylor cone will be observed any more during the experiment as the electrospinning will take place from within the needle.

Table I shows that steady state electrospinning could be established for a limited combination of process condition (wt% PA 6 and volume fraction FA/AA) only. There exists a so-called "steady state window," represented by the white cells, which is bordered by a gray and a black region for which not a single combination of electrospinning parameters could be obtained that resulted in steady state electrospinning of PA 6 nanofibres.

The steady state window is the combined result of different parameters that play a role in the electrospinning process: the surface tension, the viscosity, the dielectric constant of the solvent mixture, the solidification process, and the solubility of the PA in the solvent mixture determine the borders of the steady state window. This will be explained later.

The black region represents those solvent mixtures where PA 6 did not dissolve completely. The solvent mixtures in this region contain a high-volume percentage of acetic acid, which does not dissolve PA 6.

The light gray region is the region where although the PA 6 dissolves completely in the solvent mixture, no steady state electrospinning is possible. This region can be divided roughly in three different regions: left, below, and above the steady state window.

When looking at the region left of the steady state window, it consists of solutions with a high percentage (>66 v%) of formic acid. These solutions can be electrospun, but not under steady state condition. The Taylor cone will be unstable or droplets will be ejected from the needle. The main reason for this may be found in the relatively high dielectric constant of formic acid (57.2 at 25°C).[14] The high-dielectric constant of formic acid results from its high polarity and determines largely the charge distribution in the jet. The polar solvent will reorient as a function of the intensity and the direction of the electrical field lines.[15] This reorientation of formic acid is position dependent during electrospinning because at each position the electrical field intensity and the formic acid concentration are different. This may explain formation of droplets that prevent the system from obtaining a steady state condition.

The region below the steady state window consists of solutions with >20 wt% PA 6. During electrospinning, solidification occurs very rapidly, resulting in the deposition of PA 6 at the needle tip and a gradual blocking of the needle tip, eventually leading to an unstable Taylor cone. No steady state electrospinning is obtained in this region because of the too fast solidification process.

The region above the steady state window is not delineated by a single concentration of PA 6. Looking at the steady state window, the solvent mixture with 33 v% AA is able to electrospin in steady state starting from 15 wt%. The solvent mixture with 50 v% AA is however able to electrospin in steady state starting already from 13 wt%. The difference might be explained by a combined effect of the dielectric

TABLE II
Average Diameters for PA 6 Nanofibres Electrospun from a 50/50 (v/v%) Mixture of Formic Acid and Acetic Acid under Steady State Conditions with TCD 6 cm and 20 kV

PA 6 content (wt%)	Fibre diameter (nm)		Flow rate (ml h^{-1})
	15% RH	63% RH	
13	207	124	1.4
15	318	137	1.9
16	361	156	2.1
17	394	190	2.1
18	422	206	2.1
19	642	221	2.2

constant, the viscosity, and the surface tension of the solution. Acetic acid has a much lower dielectric constant than acetic acid (6.6 at 25°C).[14] The higher the formic acid content, the higher the dielectric constant and the more the electric field pulls at the polymeric solution. If this is not compensated by a higher viscosity of the polymeric solution, the polymeric jet will break and end up in polymeric droplets at the collector. So when the PA 6 content is less than the border value, the viscosity is too low to electrospin in steady state: for these solutions only unstable Taylor cones are observed for all the possible combinations of the process parameters. The surface tension of the mixture FA/AA also decreases with increasing acetic acid concentration (FA 38.17 mN m^{-1}, AA 27.08 mN m^{-1}).[14] A decreasing surface tension facilitates the formation of steady Taylor cones at lower viscosity or thus lower polymer concentration. A similar behavior was observed for electrospinning of chitosan from water/acetic acid solutions.[16]

Within the steady state window, the steady state solution flow rates vary with the solution composition. With increasing PA 6 content and acetic acid fraction, the polymer solution flow rate that results in steady state electrospinning is higher. It must be noted that in the available literature,[17–19] the flow rates for electrospinning PA 6 are around 1 mL h^{-1}. This means that the highest flow rates observed in this work are nearly an order of magnitude higher.

When looking at the 50/50 solvent mixture, the steady state solution flow rates increase from 1.5 mL h^{-1} to 7.5 mL h^{-1} between 13 wt% and 19 wt% of PA 6. The only difference is actually the amount of polyamide in solution. The explanation of the different steady state flow rate lies in the solvent mixture. The addition of acetic acid actually increases the boiling point of the FA/AA mixture.[20] So, when evaporation occurs during electrospinning, the evaporation of formic acid will lead to an enrichment in AA. However, in more concentrated PA 6 solutions, more formic acid is needed to keep the amide functions dissolved, so the limit of solubility is nearer. When the solubility limit is reached through evaporation of formic acid, the fibers solidify. This occurs faster for solutions with a high PA 6 content, stabilizing the Taylor cone (and thus the process itself) and allowing the increase in flow rate.

The same effect can be seen in Table I by looking at the change in steady state solution flow rate for a horizontal line (constant PA 6 content). It is to be noted that for a PA 6 content in solution, e.g., 19 wt%, with increasing acetic acid content in the solvent mixture, a higher flow rate can be obtained. The higher flow rates can be explained by the decrease of the formic acid fraction. As already pointed out, formic acid is the solvent that keeps the polyamide dissolved. When the fraction of formic acid is lower, the solubility limit is reached faster, and allows the flow rate to be higher.

Table I gives the steady state window for a specific combination of two process parameters: a TCD of 6 cm and an applied voltage of 30 kV. It must be specified that if either of these process parameters is changed, the flow rate that results in steady state electrospinning will also change. However, for all the solution mixtures that can be spun under steady state conditions, similar findings occur: if the applied voltage is lower, the flow rate that results in steady state will also be lower. This can for instance be seen in Table II, where all parameters are the same as in Table I, except for the voltage, which is reduced to 20 kV. This means that the electric field strength (kV cm^{-1}) is lower. The steady state flow rates are reduced by this. If the TCD is higher and the applied voltage stays the same, the expected flow rate that results in steady state will also be lower. It is also observed that the steady state window is the largest for both the polymer content and the solvent mixture with the process parameters of 30 kV and 6 cm (Table I). The steady state window also depends on the molar mass of the PA 6 used, as this will affect (mainly) the viscosity and the solubility.

In conclusion, this first part shows that the innovative FA/AA solvent mixture is the key to electrospinning PA 6 nanofibres under steady state conditions, which is a primary requirement for reproducibly making the samples discussed in the next section.

Analysis and morphologic study of PA 6 nanofibres

The morphology of the electrospun PA 6 is studied using SEM, whereas their thermal behavior is studied with differential scanning calorimetry (DSC). The influence of two electrospinning parameters is studied in more detail: the initial content of PA 6 and the RH while electrospinning. These two

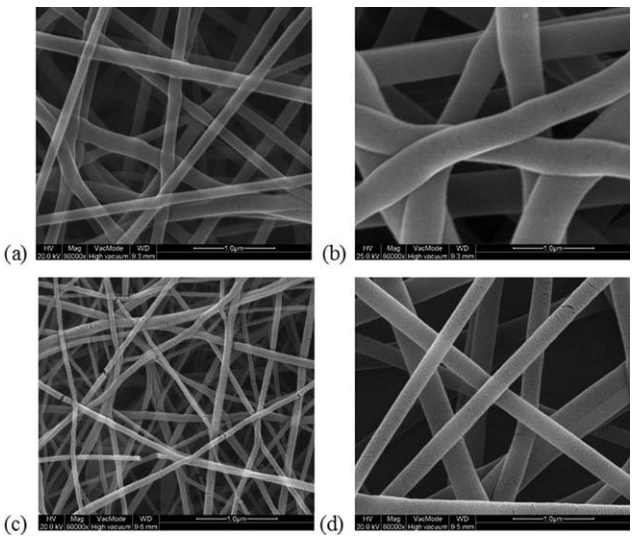

Figure 2 SEM images of PA 6 nanofibres electrospun from a 50/50 (v/v%) mixture of formic acid and acetic acid (magnification: 80.000×). (a) 13 wt% PA 6, 15% RH (b) 19 wt% PA 6, 15% RH (c) 13 wt% PA 6, 63% RH (d) 19 wt% PA 6, 63% RH.

parameters were selected, because they have the most significant impact on the average fiber diameter and thus on the final properties of the material. All other parameters were kept as constant as possible, with a tip to collector distance of 6 cm and an applied voltage of 20 kV. The solvent mixture consisted of 50 v% acetic acid. The flow rate is altered to electrospin in steady state conditions (Table II). Figure 2 shows typical SEM images for electrospun PA 6 nanofibres obtained for different PA 6 contents and at different RH values.

The standard deviation of the average nanofibre diameter is always ~ 10%. The polyamide content has a high influence on the resulting average fiber diameter. It ranges from 200 to 640 nm, when it is spun in a RH of 15% and from 124 to 221, when the RH is 63%. This is due to the higher viscosity of the polymeric solutions and the faster solidification process at higher polymer content, resulting in thicker nanofibres.

The results in Table II show that the RH has a major effect on the average fiber diameter: increasing the RH from 15% RH to 63% RH decreases the fiber diameter by roughly a factor 2. An earlier explanation[10] claimed that the solvent evaporation rate was the main reason for this effect. That article describes however electrospinning with a water-based system. This explanation should not hold in case of the FA/AA solvent mixture, as the partial vapor pressure of water in the surrounding atmosphere should not influence the evaporation rate of either formic or acetic acid. Moreover, a small amount of water also does not change the FA/AA phase diagram substantially.[20]

The following alternative explanation is proposed. The electrospun solution consists of formic acid, acetic acid, and PA 6. The only difference in the two cases is the different RH. It is hypothesized that a fraction of water is taken up by the mixture from the ambient humidity while electrospinning.[21] The higher the ambient humidity, the higher the fraction of water that will be taken up immediately in the process and the higher the equilibrium moisture content in the solution.[22] This fraction of water will act as a plasticizer for PA 6. Literature states that a minor inclusion of water in polyamide results in a tremendous drop of the glass transition temperature (T_g) of the polyamide.[23] As such, the time for stretching during electrospinning will be prolonged, resulting in thinner fibers. The plasticizing effect of water could thus explain the decrease of the fiber diameter at the higher ambient humidity level.

The effect of the PA 6 content (13–19 wt%) at 15% RH on the melting profile of the nanofibres is studied with DSC (Fig. 3). All DSC heating curves show at least two different peaks at ~ 214 and 222°C. These peaks are attributed to two different crystal forms in PA 6: the γ-phase crystals (214°C) and the α-phase crystals (222°C).[24] The total melting profile shifts toward lower temperatures when the PA 6 content is increasing, with a significant decrease of the dominant peak from 224°C to 221°C.

The observed overall decrease in melting temperature at higher PA 6 contents of the solution can be attributed to less perfect crystals. The higher the initial content of PA 6, the faster the jet reaches solidification during electrospinning. Thus, there is less time for crystallization and crystal perfectioning, rendering overall less stable crystals.

A similar effect of the PA 6 content on the melting behavior occurs in nanofibres made at 63% RH

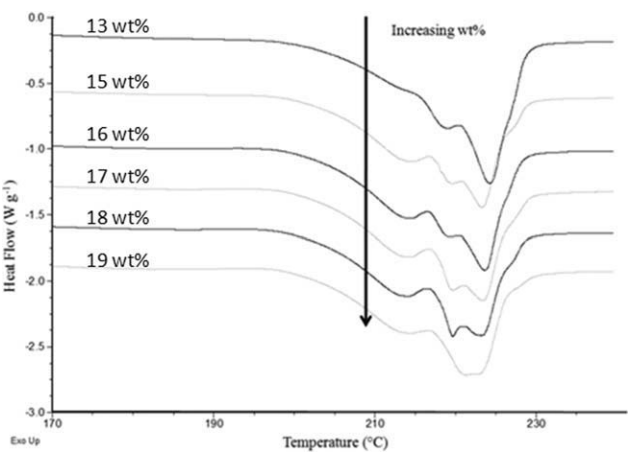

Figure 3 DSC curves of PA 6 nanofibres electrospun at 15% RH from a 50/50 (v/v%) FA/AA mixture with a PA 6 content increasing from 13 wt% to 19 wt% as indicated by the arrow (TCD: 6 cm, 20 kV).

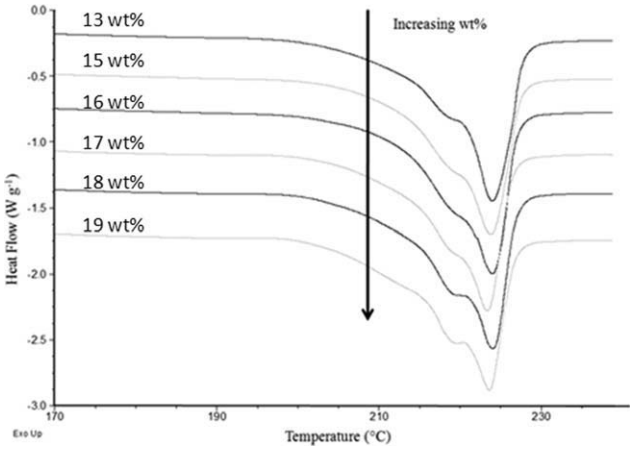

Figure 4 DSC curves of PA 6 nanofibres electrospun at 63% RH from a 50/50 (v/v%) FA/AA mixture with a PA 6 content increasing from 13 wt% to 19 wt% as indicated by the arrow (TCD: 6 cm, 20 kV).

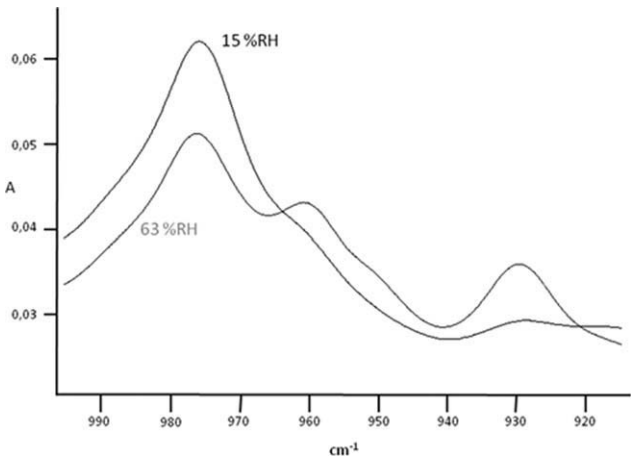

Figure 6 ATR spectra of PA 6 nanofibres electrospun from a 50/50 (v/v%) FA/AA mixture at 15% RH and 63% RH using a PA 6 content of 15 wt% (TCD: 6 cm, 20 kV).

(Fig. 4). The same explanation as earlier is valid for the results that are obtained in this figure, however, the effect is less pronounced. This is possibly due to the higher ambient humidity, which has an increased plasticising effect on the polyamide. This results also in a smaller variation of the average fiber diameter (124 to 221 nm, see Table II) compared with the variation at 15% RH (207 to 642 nm, see Table II). All samples shown in Figures 3 and 4 have a melting enthalpy of 75 ± 5 J g^{-1}. Within this range, no clear trend is seen.

Figure 5 compares the melting behavior of the electrospun PA 6 nanofibres as a function of humidity. It is clear that electrospinning at higher RH shifts the melting region to higher temperatures. This can again be linked to the influence of water as a plasticizer, with the higher amount of absorbed water during spinning at higher ambient humidity values resulting in a slower solidification and crystallization process. This is not only resulting in much thinner nanofibres but also resulting in more stable crystals within the nanofibres.

The results obtained in Figure 5 are confirmed with ATR-IR spectroscopy. The specific spectrum of PA 6 has absorptions for the gauche and trans phase at 975 cm^{-1} and 929 cm^{-1}, respectively, (Fig. 6).[25] Gauche and trans conformations are commonly linked to the more γ- and α-like crystals, respectively.[25] The results of all samples are collected in Figure 7. These measurements still have an inherent variation resulting in a lack for a systematic trend within one RH. However, when comparing the results between the different RH values, the ratio γ/α is always lower for the samples made at higher RH, thus indicating more stable crystal formation during electrospinning at higher RH. This supports the interpretation of the DSC results of Figure 5.

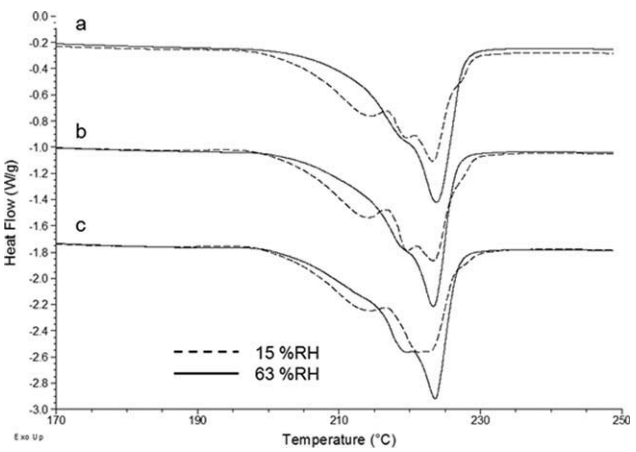

Figure 5 DSC curves of PA 6 nanofibres electrospun from a 50/50 (v/v%) FA/AA mixture at 15% RH and 63% RH with a PA 6 content of (a) 15 wt%, (b) 17 wt%, (c) 19 wt% (TCD: 6 cm, 20 kV).

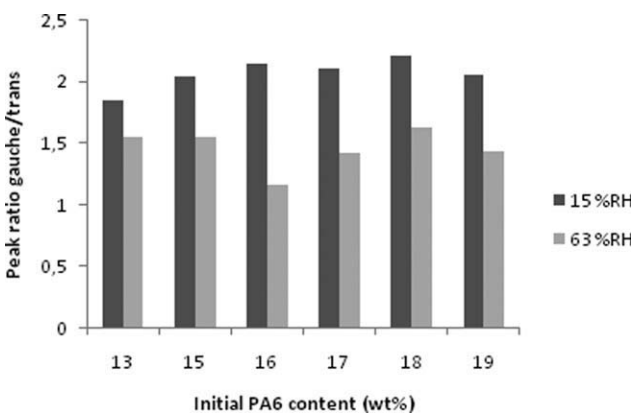

Figure 7 Peak ratios gauche/trans for the ATR spectra of PA 6 nanofibres electrospun from a 50/50 (v/v%) FA/AA mixture at 15% RH and 63% RH with different initial PA 6 content (TCD: 6 cm, 20 kV).

CONCLUSIONS

PA 6 was electrospun for the first time in steady state conditions using the mixture FA/AA. When the process parameters are set at 30 kV for the applied voltage and 6 cm for the tip-to-collector distance, only solutions with a PA 6 content between 13 wt% and 20 wt% and an acetic acid content between 33 and 50 v% are electrospinnable. The steady state window is determined and bordered as a result of the combined effect of several parameters, among which the viscosity, the dielectric constant of the solvent mixture, the solidification process, and the solubility of the PA in the solvent mixture.

The effects of the RH, often an uncontrolled ambient parameter, and the PA 6 content in the solution, a process parameter, on the morphology and thermal behavior of electrospun PA 6 nanofibres was explored. The RH proved to be determining to a large extent the diameter of the fibers but is one of the most overlooked parameters during electrospinning. Both the average diameter and the crystal morphology of the electrospun PA 6 nanofibres are markedly influenced by the RH in the air while electrospinning. When the RH increases from 15% RH to 63% RH, the average diameter of the nanofibres can decrease up to three times. This decrease is attributed to the plasticizing effect of water on PA 6. Because of the plasticizing effect of water, the polymer has more time for stretching and for crystallization. DSC and ATR-IR measurements support this explanation: the higher the RH, the lower the relative amount of the less stable γ-phase crystals.

This article contributes to the better understanding of the fundamental principles behind electrospinning—especially steady state electrospinning—providing also detailed knowledge on the effect of an overlooked parameter in electrospinning, the RH.

References

1. Thorvaldsson, A.; Stenhamre, H.; Gatenholm, P.; Walkenstrom, P. Biomacromolecules 2008, 9, 1044.
2. Henriques, C.; Vidinha, R.; Botequim, D.; Borges, J. P.; Silva, J. J Nanosci Nanotechnol 2009, 9, 3535.
3. Lu, C.; Chen, P.; Li, J.; Zhang, Y. Polymer 2006, 47, 915.
4. Formhals, A. US. Patent., 1,975,504. 1934.
5. Cooley, J. US. Patent., 692631.1902.
6. Lushnikov, A. J Aerosol Sci 1997, 28, 545.
7. Sell, S. A.; Bowlin, G. L. J Mater Chem 2008, 18, 260.
8. Li, L.; Frey, M. W.; Green, T. B. J Eng Fibers Fabrics 2006, 1, 1.
9. Lee, S.; Obendorf, S. Text Res J 2007, 77, 696.
10. De Vrieze, S.; Westbroek, P.; Van Camp, T.; De Clerck, K. J Appl Polym Sci 2010, 115, 837.
11. Dersch, R.; Liu, T.; Schaper, K.; Greiner, A.; Wendorff, J. J Polym Sci A 2003, 41, 545.
12. Jose, M.; Steinert, B.; Thomas, V.; Dean, D.; Abdalla, M.; Price, G.; Janowski, G. Polymer 2007, 48, 1096.
13. De Vrieze, S.; Van Camp, T.; Nelvig, A.; Hagstrom, B.; Westbroek, P.; De Clerck, K. J Mater Sci 2009, 44, 1357.
14. Dean, J. Lange's Handbook of Chemistry, 15th ed.; McGraw-Hill: New York, 1998.
15. Fang, Z. X.; Zhang, L.; Han, T.; Hu, P. Acta Polymerica Sinica 2004, 8, 500.
16. Geng, X.; Kwon, O.; Jang, J. Biomaterials 2005, 26, 5427.
17. Lei, L.; Bellan, L.; Craighead, H.; Frey, M. Polymer 2006, 47, 6208.
18. Cai, Y.; Li, Q.; Wei, Q.; Wu, Y.; Song, L.; Hu, Y. J Mater Sci 2008, 43, 6132.
19. Scampicchio, M.; Bulbarello, A.; Arecchi, A.; Mannino, S. Electrochem Commun 2008, 10, 991.
20. Wisniak J, Tamir A. J of Chem and Engineering Data 1977, 22, 253.
21. Pillay, S.; Vaidya, U.; Janowski, G. Compos Sci Technol 2009, 69, 839.
22. Low, H. Y.; Liu, T. X.; Loh, W. W. Polym Int 1973 2004, 53.
23. Batzer, H.; Kreibich, U. Polym Bull 1981, 5, 585.
24. Yang, Y.; Zhidong, J.; Qiang, L.; Zhicheng, G. IEEE Trans Dielectr Electr Insul 2006, 13, 580.
25. Wu, Q.; Liu, X.; Berglund, L. Polymer 2002, 43, 2445.